Non-Darcian-Bènard Double Diffusive Magneto-Marangoni Convection in a Two Layer System with Constant Heat Source/Sink

N. Manjunatha [1*], R. Sumithra [2]

[1]*Department of Mathematics, School of Applied Sciences, REVA University, Bengaluru, Indi*
[2]*Department of UG, PG Studies & Research in Mathematics, Government Science College Autonomous, Bengaluru, India*

Abstract

The problem of non-Darcian-Bènard double diffusive magneto-Marangoni convection is considered in a horizontal infinite two layer system. The system consists of a two-component fluid layer placed above a porous layer, saturated with the same fluid with a constant heat sources/sink in both the layers, in the presence of a vertical magnetic field. The lower porous layer is bounded by rigid boundary, while the upper boundary of the fluid region is free with the presence of Marangoni effects. The system of ordinary differential equations obtained after normal mode analysis is solved in a closed form for the eigenvalue and the Thermal Marangoni Number (TMN) for two cases of Thermal Boundary Combinations (TBC); these are type (i) Adiabatic-Adiabatic and type (ii) Adiabatic-Isothermal. The corresponding two TMNs are obtained and the impacts of the porous parameter, solute Marangoni number, modified internal Rayleigh numbers, viscosity ratio, and the diffusivity ratios on the non-Darcian-Bènard double diffusive magneto - Marangoni convection are studied in detail.

Keywords: Heat source/sink, Double diffusive convection, Marangoni number, modified internal Rayleigh number, thermal ratio.

Introduction

Double diffusive convection (DDC) is a type of convection, which consists of double density gradients diffusing at varied rates. DDC commonly occurs in natural processes, like those taking place in sea water and the mantle flow in the Earth's crust, and has lots of engineering geothermal applications; for example, contaminant transport in saturated soils, food processing, and spread of toxins. It also appears in solar ponds and crystal growth industries. In crystal growth industries, double diffusive Marangoni convection (DDMC) plays an important role in the production of pure crystals. Applying magnetic field on DDMC can exert outstanding outcomes in crystal growth industries.

Steady conjugate double-diffusive natural convective heat and mass transfer in a two-dimensional variable porosity layer sandwiched between two walls was studied numerically by Al-Farhany and Turan [1]. The linear and nonlinear stability of double diffusive convection in a layer of couple stress fluid–saturated porous medium was theoretically investigated by Shivakumara *et al.* [2]. A numerical study of double-diffusive natural convective heat and mass transfer in an inclined rectangular cavity filled with a porous medium was conducted by Al-Farhany and Turan [3]. Mehmood *et al.* [4] explored the unsteady flow of viscous nanofluid driven by an inclined stretching sheet for the effect of a

---

*Email: manjunatha.n@reva.edu.in

non-uniform heat source/sink in a thermally and solutally stratified magnetonanofluid, using the RK4 method with the shooting technique. Al-Farhany and Turan [5] experimentally investigated the mixed convection in a square enclosure partitioned in two layers. The results showed that the effect of cylinder rotation was exerted around the cylinder only. Mixed convection heat transfer of nanofluid in a lid-driven porous medium square enclosure with several pairs of heat source-sinks was numerically simulated by Munshi *et al*. [6] using the finite element method. Ahmadpour *et al*. [7] studied the natural convection of a non-Newtonian ferrofluid in a porous elliptical enclosure in the presence of a non-uniform magnetic field. The results showed that, by applying the magnetic field via a wire, the overall heat transfer rate increased significantly. The onset of double diffusive magneto Marangoni convection in a two-layer system, comprising incompressible two components, was studied by Komala and Sumithra [8] using the regular perturbation technique for uniform and nonuniform salinity gradients.

Recently, the effect of heat source/sink on MHD free convection flow in a channel filled with nanofluid in the existence of induced magnetic field was studied by Jha and Samaila [9]. Kannan and Pullepu [10] studied the effects for chemical reaction, the heat source/sink, Schmidt number, and Prandtl number on double diffusion natural convective flow along a vertically inclined infinite plate. The governing non-dimensional equations were solved using iterative tri-diagonal implicit finite-difference scheme. Anurag *et al*. [11] studied the influence of Newtonian heating/cooling in the presence of heat source/sink on laminar free convective flow in a vertical annular permeable region. The closed-form analytical solutions of the governing equations were obtained for two different cases of internal heat generation/absorption. Sumithra *et al*. [12, 13] and Manjunatha and Sumithra [14] studied the effects of constant heat source / sink and temperature gradients on composite layer with and without magnetic field. They obtained the closed form of solution to thermal Marangoni number for three different temperature gradients. Sumithra and Venkatraman [15] studied the problem of Bènard Marangoni convection in a composite layer, comprised of an incompressible couple stress fluid, for adiabatic and isothermal boundaries using an exact technique.

In this paper, the problem of non-Darcy-Bènard double diffusive magneto Marangoni convection is investigated in a horizontally infinite two layer system. The system consists of a two-component fluid layer above a porous layer, saturated with the same fluid, for Darcy-Brinkmann model with constant heat sources in both the layers under microgravity condition. The lower boundary of the porous region is rigid, while the upper boundary of the fluid region is free with the presence of Marangoni effects. The system of ordinary differential equations obtained after normal mode analysis is solved in a closed form for the eigenvalue and TMN for two types of TBC; type (i) Adiabatic-Adiabatic and type (ii) Adiabatic-Isothermal. The corresponding two thermal Marangoni numbers M_{t1} & M_{t2} are obtained and the impacts of the different parameters are investigated in detail.

Mathematical formulation of the problem

Consider a horizontal double component, an electrically conducting fluid saturated isotropic sparsely packed porous layer of thickness d_m, underlying a two component fluid layer of thickness d, with an imposed magnetic field of intensity H_0 in the vertical z-direction and heat sources Φ_m and Φ, respectively. The lower surface of the porous layer is rigid and the upper surface of the fluid layer is free with the presence of surface tension effects, depending on temperature and concentration. A Cartesian coordinate system is chosen that originates at the interface between the porous and fluid layers and the z-axis, in the vertically upward direction. The basic equations for the fluid and porous layers, respectively, governing such a system are:

$$\nabla.\vec{V} = 0 \tag{1}$$

$$\nabla.\vec{H} = 0 \tag{2}$$

$$\rho_0 \left[\frac{\partial \vec{V}}{\partial t} + \left(\vec{V}.\nabla \right)\vec{V} \right] = -\nabla P + \mu \nabla^2 \vec{V} + \mu_p \left(\vec{H}.\nabla \right)\vec{H} \tag{3}$$

$$\frac{\partial T}{\partial t} + \left(\vec{V}.\nabla \right)T = \kappa \nabla^2 T + \Phi \tag{4}$$

$$\frac{\partial C}{\partial t} + \left(\vec{V}.\nabla \right)C = \kappa_c \nabla^2 C \tag{5}$$

$$\frac{\partial \vec{H}}{\partial t} = \nabla \times \vec{V} \times \vec{H} + \nu \nabla^2 \vec{H} \tag{6}$$

$$\nabla_m.\vec{V}_m = 0 \tag{7}$$

$$\nabla_m.\vec{H} = 0 \tag{8}$$

$$\rho_0 \left[\frac{1}{\phi} \frac{\partial \vec{V}}{\partial t} + \frac{1}{\phi^2} \left(\vec{V}_m.\nabla_m \right)\vec{V}_m \right] = -\nabla_m P_m - \frac{\mu}{K} \vec{V}_m + \mu_m \nabla_m^2 \vec{V}_m + \mu_p \left(\vec{H}.\nabla_m \right)\vec{H} \tag{9}$$

$$A \frac{\partial T_m}{\partial t} + \left(\vec{V}_m.\nabla_m \right)T_m = \kappa_m \nabla_m^2 T_m + \Phi_m \tag{10}$$

$$\phi \frac{\partial C_m}{\partial t} + \left(\vec{V}_m.\nabla_m \right)C_m = \kappa_{cm} \nabla_m^2 C_m \tag{11}$$

$$\phi \frac{\partial \vec{H}}{\partial t} = \nabla_m \times \vec{V}_m \times \vec{H} + \nu_{em} \nabla_m^2 \vec{H} \tag{12}$$

where for the fluid layer, $\vec{V}$ is the velocity vector, ρ_0 is the fluid density, t is time, μ is the fluid viscosity, $P = p + \frac{\mu_p H^2}{2}$ is the total pressure, $\vec{H}$ is the magnetic field, T is the temperature, κ is the thermal diffusivity of the fluid, $\nu = \frac{1}{\mu_p \sigma}$ is the magnetic viscosity, and μ_p is the magnetic permeability. For the porous layer, ϕ is the porosity, μ_m is the effective viscosity of the fluid in the porous layer, K is the permeability of the porous medium, A is the ratio of heat capacities, κ_m is the thermal diffusivity, $\nu_{em} = \frac{\nu}{\phi}$ is the effective magnetic viscosity, and the subscript 'm' denotes the quantities in the porous layer.

The aim of this paper is to investigate the stability of a quiescent state to infinitesimal perturbations superposed on the basic state. The basic state of the liquid being quiescent is described by

Fluid layer:

$$\vec{V} = 0, P = P_b(z), T = T_b(z), C = C_b(z), \vec{H} = H_0(z) \tag{13}$$

Porous layer:

$$\overrightarrow{V_m} = 0, P_m = P_{mb}(z_m), T_m = T_{mb}(z_m), C_m = C_{mb}(z_m), \vec{H} = H_0(z_m) \tag{14}$$

The temperature distributions in the basic state are obtained by

$$T_b(z) = \frac{-\Phi z(z-d)}{2\kappa} + \frac{(T_u - T_0)z}{d} + T_0 \qquad 0 \le z \le d \tag{15}$$

$$T_{mb}(z_m) = \frac{-\Phi_m z_m(z_m + d_m)}{2\kappa_m} + \frac{(T_0 - T_l)z_m}{d_m} + T_0 \qquad -d_m \le z_m \le 0 \tag{16}$$

The concentration distributions in the basic state are obtained by

$$C_b(z) = C_0 - \frac{(C_0 - C_u)z}{d} \qquad\qquad 0 \le z \le d \tag{17}$$

$$C_{mb}(z_m) = C_0 - \frac{(C_l - C_0)z_m}{d_m} \qquad -d_m \le z_m \le 0 \tag{18}$$

where $T_0 = \dfrac{\kappa d_m T_u + \kappa_m d T_l}{\kappa d_m + \kappa_m d} + \dfrac{d d_m (\Phi_m d_m + \Phi d)}{2(\kappa d_m + \kappa_m d)}$ and $C_0 = \dfrac{\kappa_c d_m C_u + \kappa_c d_m C_l}{\kappa_c d_m + \kappa_c d_m}$ are the interface temperature and concentration, respectively.

To investigate the stability of the basic state, infinitesimal disturbances are superimposed, ass follows.

Fluid layer:

$$\vec{V} = \vec{V}', P = P_b + P', T = T_b(z) + \theta, C = C_b(z) + S, \vec{H} = H_0(z) + \vec{H}' \tag{19}$$

Porous layer:

$$\vec{V}_m = \vec{V}_m', P_m = P_{mb} + P_m', T_m = T_{mb}(z_m) + \theta_m, C_m = C_{mb}(z_m) + S_m, \vec{H} = H_0(z_m) + \vec{H}' \tag{20}$$

Following the standard linear stability analysis procedure and assuming that the principle of exchange of stability holds (Manjunatha and Sumithra [14]), we arrive at the following stability equations:

in $0 \le z \le 1$

$$(D^2 - a^2)^2 W(z) = Q D^2 W(z) \tag{21}$$

$$(D^2 - a^2)\theta(z) + [1 + R_I^*(2z - 1)]W(z) = 0 \tag{22}$$

$$\tau(D^2 - a^2)S(z) + W(z) = 0 \tag{23}$$

in $-1 \le z_m \le 0$

$$[(D_m^2 - a_m^2)\hat{\mu}\beta^2 - 1](D_m^2 - a_m^2)W_m(z_m) = Q_m \beta^2 D_m^2 W_m(z_m) \tag{24}$$

$$(D_m^2 - a_m^2)\theta_m(z_m) + [1 + R_{Im}^*(2z_m + 1)]W_m(z_m) = 0 \tag{25}$$

$$\tau_{pm}(D_m^2 - a_m^2)S_m(z_m) + W_m(z_m) = 0 \tag{26}$$

In the above equations, Q, $R_I^* = \dfrac{R_i}{2(T_0 - T_u)}$, $R_i = \dfrac{\Phi d^2}{\kappa}$, and $\tau = \dfrac{\kappa_c}{\kappa}$ are namely the Chandrasekhar number, the modified internal Rayleigh number, the internal Rayleigh number, and the solute-thermal diffusivity ratio, respectively for the fluid layer. While, $\hat{\mu} = \dfrac{\mu_m}{\mu}$,

$\beta = \sqrt{\dfrac{K}{d_m^2}}$, Q_m, $R_{Im}^* = \dfrac{R_{im}}{2(T_l - T_0)}$, $R_{im} = \dfrac{\Phi_m d_m^2}{\kappa_m}$, and $\tau_{pm} = \dfrac{\kappa_{cm}}{\kappa_m}$ are namely the viscosity ratio, the porous parameter, the Chandrasekhar number, the modified internal Rayleigh number, the internal Rayleigh number, and the solute-thermal diffusivity ratio, respectively, for the porous layer. $W(z)$ & $W_m(z_m)$ are the vertical velocities, $\theta(z)$ & $\theta_m(z_m)$ are the temperature distributions, and $S(z)$ & $S_m(z_m)$ are the concentration distributions in the fluid and porous layers, respectively, while a and a_m are the horizontal wave numbers. Since the horizontal wave numbers must be the same for the composite layers, so that we have $\dfrac{a}{d} = \dfrac{a_m}{d_m}$ and

hence $a_m = \hat{d}a$, where $\hat{d} = \dfrac{d_m}{d}$ is the depth ratio.

Boundary Conditions

The suitable velocity boundary conditions are nondimensionalized and then subjected to normal mode analysis; they are

$$D^2 W(1) + M_t a^2 \theta(1) + M_s a^2 S(1) = 0 \tag{27}$$

$$W(1) = 0, W_m(-1) = 0, D_m W_m(-1) = 0, \hat{T} W(0) = W_m(0),$$

$$\hat{T}\hat{d} D W(0) = D_m W_m(0), \ \hat{T} d^2 (D^2 + a^2) W(0) = \hat{\mu}(D_m^2 + a_m^2) W_m(0),$$

$$\hat{T} d^3 \beta^2 (D^3 - 3a^2 D) W(0) = -D_m W_m(0) + \hat{\mu}\beta^2 (D_m^3 - 3a_m^2 D_m) W_m(0) \tag{28}$$

where $\hat{T} = \dfrac{T_l - T_0}{T_0 - T_u}$ is the thermal ratio, $M_t = -\dfrac{\partial \sigma_t}{\partial T} \dfrac{(T_0 - T_u)d}{\mu\kappa}$ is the TMN,

$M_s = -\dfrac{\partial \sigma_t}{\partial C} \dfrac{(C_0 - C_u)d}{\mu\kappa}$ is the solute Marangoni number, and σ_t is the surface tension.

Method of Solution

The solutions of $W(z)$ and $W_m(z_m)$ are obtained by solving (21) and (24) using the velocity boundary condition (28), as follows

$$W(z) = A_1[\cosh \delta z + a_1 \sinh \delta z + a_2 \cosh \zeta z + a_3 \sinh \zeta z] \tag{29}$$

$$W_m(z_m) = A_1[a_4 \cosh \eta_m z_m + a_5 \sinh \eta_m z_m + a_6 \cosh \psi_m z_m + a_7 \sinh \psi_m z_m] \tag{30}$$

where $\delta = \dfrac{\sqrt{Q} + \sqrt{Q + 4a^2}}{2}$, $\zeta = \dfrac{\sqrt{Q} - \sqrt{Q + 4a^2}}{2}$,

$\eta_m = \sqrt{\dfrac{E + \sqrt{E^2 - 4F}}{2}}, \psi_m = \sqrt{\dfrac{E - \sqrt{E^2 - 4F}}{2}}$,

$E = \dfrac{(2\hat{\mu}\beta^2 a_m^2 + 1 + Q_m \beta^2)}{\hat{\mu}\beta^2}, F = \dfrac{(a_m^2 + a_m^4 \hat{\mu}\beta^2)}{\hat{\mu}\beta^2}$,

$a_1 = \dfrac{-1}{\delta_{14}}(a_6 \delta_{15} + a_7 \delta_{16} + \delta_{17}), a_2 = a_6 \delta_5 + \delta_6, a_3 = \dfrac{1}{\delta_9}(a_1 \delta_{10} + a_7 \delta_{11})$,

$a_4 = \delta_7 + a_6 \delta_8, a_5 = a_1 \delta_{12} + a_7 \delta_{13}, a_6 = \dfrac{\delta_{23}\delta_{25} - \delta_{26}\delta_{22}}{\delta_{25}\delta_{21} - \delta_{24}\delta_{22}}$,

$a_7 = \dfrac{\delta_{23}\delta_{24} - \delta_{26}\delta_{21}}{\delta_{24}\delta_{22} - \delta_{25}\delta_{21}}, \delta_1 = \hat{T}\beta^2 d^3 (\delta^3 - 3a^2 \delta), \delta_2 = \hat{T}\beta^2 d^3 (\zeta^3 - 3a^2 \zeta)$,

$\delta_3 = \hat{\mu}\beta^2 (\eta_m^3 - 3a_m^2 \eta_m) - \eta_m, \delta_4 = \hat{\mu}\beta^2 (\psi_m^3 - 3a_m^2 \psi_m) - \psi_m$,

$\delta_5 = \dfrac{\hat{\mu}[(\psi_m^2 + a_m^2) - \hat{T}(\eta_m^2 + a_m^2)]}{\hat{T}d^2(\zeta^2 + a^2) - \hat{\mu}\hat{T}(\eta_m^2 + a_m^2)}, \qquad \delta_6 = \dfrac{\hat{\mu}(\eta_m^2 + a_m^2) - d^2(\delta^2 + a^2)}{d^2(\zeta^2 + a^2) - \hat{\mu}(\eta_m^2 + a_m^2)}$,

$\delta_7 = \hat{T}(1 + \delta_6), \delta_8 = \hat{T}\delta_5 - 1, \delta_9 = \delta_2 - \dfrac{\hat{T}\hat{d}\zeta\delta_3}{\eta_m}, \delta_{10} = -\delta_1 + \dfrac{\hat{T}\hat{d}\delta\delta_3}{\eta_m}$,

$\delta_{11} = \delta_4 - \dfrac{\psi_m \delta_3}{\eta_m}, \delta_{12} = \dfrac{1}{\eta_m}(\hat{T}\hat{d}\delta + \dfrac{\zeta\delta_{10}}{\delta_9}), \delta_{13} = \dfrac{1}{\eta_m}(\dfrac{\hat{T}\hat{d}\zeta\delta_{11}}{\delta_9} - \psi_m)$,

$\delta_{14} = \sinh \delta + \dfrac{\delta_{10} \sinh \zeta}{\delta_9}, \delta_{15} = \delta_5 \cosh \zeta, \delta_{16} = \dfrac{\delta_{11} \sinh \zeta}{\delta_9}$,

$\delta_{17} = \delta_6 \cosh \zeta + \cosh \delta, \delta_{18} = \dfrac{\delta_{12}\delta_{15}}{\delta_{14}}, \delta_{19} = \dfrac{\delta_{12}\delta_{16}}{\delta_{14}} + \delta_{13}, \delta_{20} = \dfrac{\delta_{12}\delta_{17}}{\delta_{14}}$,

$$\delta_{21} = \delta_8 \cosh\eta_m - \delta_{18}\sinh\eta_m + \cosh\psi_m,$$

$$\delta_{22} = -\delta_{19}\sinh\eta_m - \sinh\psi_m, \delta_{23} = \delta_{20}\sinh\eta_m - \delta_7\cosh\eta_m,$$

$$\delta_{24} = -\eta_m\delta_8\sinh\eta_m - \delta_{18}\eta_m\cosh\eta_m - \psi_m\sinh\psi_m, \qquad \delta_{25} = -\eta_m\delta_{19}\cosh\eta_m + \psi_m\cosh\psi_m,$$

$$\delta_{26} = \delta_{20}\eta_m\cosh\eta_m + \delta_7\eta_m\sinh\eta_m$$

We solve equations (23) and (26) for the salinity distributions $S(z)$ and $S_m(z_m)$ using the following salinity/concentration boundary conditions

$$DS(1) = 0, S(0) = \hat{S}S_m(0), DS(0) = D_m S_m(0), D_m S_m(-1) = 0 \tag{31}$$

where $\hat{S} = \dfrac{C_l - C_0}{C_0 - C_u}$ is the solutal ratio. The concentration distributions $S(z)$ and $S_m(z_m)$ are

obtained using the concentration boundary conditions (31), as follows

$$S(z) = A_1[c_9\cosh az + c_{10}\sinh az + f_1(z)] \tag{32}$$

$$S_m(z_m) = A_1[c_{11}\cosh a_m z_m + c_{12}\sinh a_m z_m + f_{m1}(z_m)] \tag{33}$$

where

$$f_1(z) = \frac{-1}{\tau}\left[\frac{\cosh\delta z + a_1\sinh\delta z}{\delta^2 - a^2} + \frac{a_2\cosh\zeta z + a_3\sinh\zeta z}{\zeta^2 - a^2}\right]$$

$$f_{m1}(z_m) = \frac{-1}{\tau_{pm}}\left[\frac{a_4\cosh\eta_m z_m + a_5\sinh\eta_m z_m}{\eta_m^2 - a_m^2} + \frac{a_6\cosh\psi_m z_m + a_7\sinh\psi_m z_m}{\psi_m^2 - a_m^2}\right]$$

$$c_9 = \hat{S}c_{11} + \Delta_{100} + \Delta_{101}, c_{10} = \frac{1}{a}(c_{12}a_m + \Delta_{102} + \Delta_{103}),$$

$$c_{11} = \frac{\Delta_{108}a_m\cosh a_m - \Delta_{107}\Delta_{105}}{a_m\sinh a_m\Delta_{107} + \Delta_{106}a_m\cosh a_m}, c_{12} = \frac{\Delta_{105}\Delta_{106} + a_m\sinh a_m\Delta_{108}}{a_m\sinh a_m\Delta_{107} + \Delta_{106}a_m\cosh a_m}$$

$$\Delta_{100} = \frac{-\hat{S}}{\tau_{pm}}\left[\frac{a_4}{\eta_m^2 - a_m^2} + \frac{a_6}{\psi_m^2 - a_m^2}\right], \Delta_{101} = \frac{1}{\tau}\left[\frac{1}{\delta^2 - a^2} + \frac{a_2}{\zeta^2 - a^2}\right]$$

$$\Delta_{102} = \frac{-1}{\tau_{pm}}\left[\frac{\eta_m a_5}{\eta_m^2 - a_m^2} + \frac{\psi_m a_7}{\psi_m^2 - a_m^2}\right], \Delta_{103} = \frac{1}{\tau}\left[\frac{a_1\delta}{\delta^2 - a^2} + \frac{a_3\zeta}{\zeta^2 - a^2}\right],$$

$$\Delta_{104} = \frac{1}{\tau}\left[\frac{(\sinh\delta + a_1\cosh\delta)\delta}{\delta^2 - a^2} + \frac{(a_2\sinh\zeta + a_3\cosh\zeta)\zeta}{\zeta^2 - a^2}\right],$$

$$\Delta_{105} = \frac{1}{\tau_{pm}}\left[\frac{\eta_m(-a_4\sinh\eta_m + a_5\cosh\eta_m)}{\eta_m^2 - a_m^2} + \frac{\psi_m(-a_6\sinh\psi_m + a_7\cosh\psi_m)}{\psi_m^2 - a_m^2}\right],$$

$$\Delta_{106} = \hat{S}a\sinh a, \Delta_{107} = a_m\cosh a, \Delta_{108} = \Delta_{104} - (\Delta_{100} + \Delta_{101})a\sinh a - (\Delta_{102} + \Delta_{103})\cosh a$$

Thermal Marangoni number
Type (i): Adiabatic-Adiabatic (A-A) Boundaries
We solve equations (22) and (25) for the temperature distributions $\theta(z)$ and $\theta_m(z_m)$ using the following temperature boundary conditions, where both the boundaries are adiabatic and the heat and heat flux are continuous at the interface:

$$D\theta(1) = 0, \theta(0) = \hat{T}\theta_m(0), D\theta(0) = D_m\theta_m(0), D_m\theta_m(-1) = 0 \tag{34}$$

The temperature distributions $\theta(z)$ and $\theta_m(z_m)$ are obtained by using the temperature boundary condition (34), as follows

$$\theta(z) = A_1[c_1\cosh az + c_2\sinh az + g_1(z)] \tag{35}$$

$$\theta_m(z_m) = A_1[c_3\cosh a_m z_m + c_4\sinh a_m z_m + g_{m1}(z_m)] \tag{36}$$

where

$$g_1(z) = A_1[\delta_{27} - \delta_{28} + \delta_{29} - \delta_{30}], \quad g_{m1}(z_m) = A_1[\delta_{31} - \delta_{32} + \delta_{33} - \delta_{34}]$$

$$\delta_{27} = \frac{(E_2 z + E_1)}{(\delta^2 - a^2)}(\cosh \delta z + a_1 \sinh \delta z)$$

$$\delta_{28} = \frac{2\delta E_2}{(\delta^2 - a^2)^2}(a_1 \cosh \delta z + \sinh \delta z)$$

$$\delta_{29} = \frac{(E_2 z + E_1)}{(\zeta^2 - a^2)}(a_2 \cosh \zeta z + a_3 \sinh \zeta z)$$

$$\delta_{30} = \frac{2\zeta E_2}{(\zeta^2 - a^2)^2}(a_3 \cosh \zeta z + a_2 \sinh \zeta z)$$

$$\delta_{31} = \frac{(E_{2m} z_m + E_{1m})}{(\eta_m^2 - a_m^2)}(a_4 \cosh \eta_m z_m + a_5 \sinh \eta_m z_m)$$

$$\delta_{32} = \frac{2\eta_m E_{2m}}{(\eta_m^2 - a_m^2)^2}(a_5 \cosh \eta_m z_m + a_4 \sinh \eta_m z_m)$$

$$\delta_{33} = \frac{(E_{2m} z_m + E_{1m})}{(\psi_m^2 - a_m^2)}(a_6 \cosh \psi_m z_m + a_7 \sinh \psi_m z_m)$$

$$\delta_{34} = \frac{2\psi_m E_{2m}}{(\psi_m^2 - a_m^2)^2}(a_7 \cosh \psi_m z_m + a_6 \sinh \psi_m z_m)$$

$$E_1 = R_I^* - 1, \; E_2 = -2R_I^*, \; E_{1m} = -(R_{Im}^* + 1), \; E_{2m} = -2R_{Im}^*$$

$$c_1 = c_3 \hat{T} + \Delta_2 - \Delta_3, \; c_2 = \frac{1}{a}(c_4 a_m + \Delta_4 - \Delta_5),$$

$$c_3 = \frac{\Delta_8 \Delta_{10} - \Delta_{11} \Delta_6}{-\Delta_7 \Delta_{10} - \Delta_9 \Delta_6}, \; c_4 = \frac{\Delta_8 \Delta_9 + \Delta_{11} \Delta_7}{\Delta_6 \Delta_9 + \Delta_{10} \Delta_7},$$

$$\Delta_1 = -A_1[\delta_{35} + \delta_{36} + \delta_{37} + \delta_{38}],$$

$$\delta_{35} = \frac{\delta(E_2 + E_1)}{(\delta^2 - a^2)}(a_1 \cosh \delta + \sinh \delta),$$

$$\delta_{36} = \left[\frac{E_2}{(\delta^2 - a^2)} - \frac{2\delta^2 E_2}{(\delta^2 - a^2)^2}\right](\cosh \delta + a_1 \sinh \delta),$$

$$\delta_{37} = \frac{\zeta(E_2 + E_1)}{(\zeta^2 - a^2)}(a_3 \cosh \zeta + a_2 \sinh \zeta),$$

$$\delta_{38} = \left[\frac{E_2}{(\zeta^2 - a^2)} - \frac{2\zeta^2 E_2}{(\zeta^2 - a^2)^2}\right](a_2 \cosh \zeta + a_3 \sinh \zeta),$$

$$\Delta_2 = \hat{T}\left[\frac{E_{1m} a_4}{(\eta_m^2 - a_m^2)} - \frac{2E_{2m} \eta_m a_5}{(\eta_m^2 - a_m^2)^2} + \frac{E_{1m} a_6}{(\psi_m^2 - a_m^2)} - \frac{2E_{2m} \psi_m a_7}{(\psi_m^2 - a_m^2)^2}\right],$$

$$\Delta_3 = \frac{E_1}{(\delta^2 - a^2)} - \frac{2\delta a_1 E_2}{(\delta^2 - a^2)^2} + \frac{a_2 E_1}{(\zeta^2 - a^2)} - \frac{2\zeta a_3 E_2}{(\zeta^2 - a^2)^2},$$

$$\Delta_4 = \left[\frac{E_{2m}}{(\eta_m^2 - a_m^2)} - \frac{2\eta_m^2 E_{2m}}{(\eta_m^2 - a_m^2)^2}\right]a_4 + \frac{\eta_m a_5 E_{1m}}{(\eta_m^2 - a_m^2)} + \Delta_{400}$$

$$\Delta_{400} = [\frac{E_{2m}}{(\psi_m^2 - a_m^2)} - \frac{2\psi_m^2 E_{2m}}{(\psi_m^2 - a_m^2)^2}]a_6 + \frac{\psi_m a_7 E_{1m}}{(\psi_m^2 - a_m^2)}$$

$$\Delta_5 = \frac{E_1\delta a_1 + E_2}{(\delta^2 - a^2)} - \frac{2E_2\delta^2}{(\delta^2 - a^2)^2} + \frac{E_1\zeta a_3 + E_2 a_2}{(\zeta^2 - a^2)} - \frac{2a_2 E_2\zeta^2}{(\zeta^2 - a^2)^2},$$

$$\Delta_6 = a_m \cosh a_m, \Delta_7 = a_m \sinh a_m, \Delta_8 = -[\delta_{39} + \delta_{40} + \delta_{41} + \delta_{42}]$$

$$\delta_{39} = [\frac{E_{2m}}{(\eta_m^2 - a_m^2)} - \frac{2\eta_m^2 E_{2m}}{(\eta_m^2 - a_m^2)^2}](a_4 \cosh \eta_m - a_5 \sinh \eta_m)$$

$$\delta_{40} = \eta_m \frac{(E_{1m} - E_{2m})}{(\eta_m^2 - a_m^2)}(a_5 \cosh \eta_m - a_4 \sinh \eta_m)$$

$$\delta_{41} = [\frac{E_{2m}}{(\psi_m^2 - a_m^2)} - \frac{2\psi_m^2 E_{2m}}{(\psi_m^2 - a_m^2)^2}](a_6 \cosh \psi_m - a_7 \sinh \psi_m)$$

$$\delta_{42} = \psi_m \frac{(E_{1m} - E_{2m})}{(\psi_m^2 - a_m^2)}(a_7 \cosh \psi_m - a_6 \sinh \psi_m)$$

$$\Delta_9 = \hat{T}a \sinh a, \Delta_{10} = a_m \cosh a, \Delta_{11} = \Delta_1 - a(\Delta_2 - \Delta_3)\sinh a - (\Delta_4 - \Delta_5)\cosh a$$

From the boundary condition (27), we have

$$M_t = -\left[\frac{D^2 W(1) + M_s a^2 S(1)}{a^2 \theta(1)}\right]$$

The TMN is as follows

$$M_{t1} = \frac{-(\Lambda_1 + \Lambda_2)}{a^2(c_1 \cosh a + c_2 \sinh a + \Lambda_3 + \Lambda_4)} \tag{37}$$

where

$$\Lambda_1 = \delta^2(\cosh \delta + a_1 \sinh \delta) + \zeta^2(a_2 \cosh \zeta + a_3 \sinh \zeta),$$

$$\Lambda_2 = \frac{-M_s a^2}{\tau}\left[\frac{\cosh \delta + a_1 \sinh \delta}{\delta^2 - a^2} + \frac{a_2 \cosh \zeta + a_3 \sinh \zeta}{\zeta^2 - a^2}\right],$$

$$\Lambda_3 = \frac{(E_2 + E_1)}{(\delta^2 - a^2)}(\cosh \delta + a_1 \sinh \delta) - \frac{2\delta E_2}{(\delta^2 - a^2)^2}(a_1 \cosh \delta + \sinh \delta)$$

$$\Lambda_4 = \frac{(E_2 + E_1)}{(\zeta^2 - a^2)}(a_2 \cosh \zeta + a_3 \sinh \zeta) - \frac{2\zeta E_2}{(\zeta^2 - a^2)^2}(a_3 \cosh \zeta + a_2 \sinh \zeta)$$

Type (ii): Adiabatic-Isothermal (A-I) Boundaries

We solve equations (22) and (25) for the temperature distributions $\theta(z)$ and $\theta_m(z_m)$ using the following temperature boundary conditions, where the upper boundary of the fluid layer is adiabatic and the lower boundary of the porous layer is isothermal, and at the interface, heat and heat flux are continuous:

$$D\theta(1) = 0, \theta(0) = \hat{T}\theta_m(0), D\theta(0) = D_m\theta_m(0), \theta_m(-1) = 0 \tag{38}$$

The temperature distributions $\theta(z)$ and $\theta_m(z_m)$ are obtained by using the temperature boundary conditions (38), as follows

$$\theta(z) = A_1[c_5 \cosh az + c_6 \sinh az + g_2(z)] \tag{39}$$

$$\theta_m(z_m) = A_1[c_7 \cosh a_m z_m + c_8 \sinh a_m z_m + g_{m2}(z_m)] \tag{40}$$

where

$$g_2(z) = A_1[\delta_{42} - \delta_{43} + \delta_{44} - \delta_{45}],$$

$$g_{m2}(z_m) = A_1[\delta_{46} - \delta_{47} + \delta_{48} - \delta_{49}]$$

$$\delta_{42} = \frac{(E_4 z + E_3)}{(\delta^2 - a^2)}(\cosh \delta z + a_1 \sinh \delta z)$$

$$\delta_{43} = \frac{2\delta E_4}{(\delta^2 - a^2)^2}(a_1 \cosh \delta z + \sinh \delta z)$$

$$\delta_{44} = \frac{(E_4 z + E_3)}{(\zeta^2 - a^2)}(a_2 \cosh \zeta z + a_3 \sinh \zeta z)$$

$$\delta_{45} = \frac{2\zeta E_4}{(\zeta^2 - a^2)^2}(a_3 \cosh \zeta z + a_2 \sinh \zeta z)$$

$$\delta_{46} = \frac{(E_{4m} z_m + E_{3m})}{(\eta_m^2 - a_m^2)}(a_4 \cosh \eta_m z_m + a_5 \sinh \eta_m z_m)$$

$$\delta_{47} = \frac{2\eta_m E_{4m}}{(\eta_m^2 - a_m^2)^2}(a_5 \cosh \eta_m z_m + a_4 \sinh \eta_m z_m)$$

$$\delta_{48} = \frac{(E_{4m} z_m + E_{3m})}{(\psi_m^2 - a_m^2)}(a_6 \cosh \psi_m z_m + a_7 \sinh \psi_m z_m)$$

$$\delta_{49} = \frac{2\psi_m E_{4m}}{(\psi_m^2 - a_m^2)^2}(a_7 \cosh \psi_m z_m + a_6 \sinh \psi_m z_m)$$

$$E_3 = R_I^* - 1, E_4 = -2R_I^*, E_{3m} = -(R_{Im}^* + 1), E_{4m} = -2R_{Im}^*$$

$$c_5 = c_7 \hat{T} + \Delta_{13} - \Delta_{14}, c_6 = \frac{1}{a}(c_8 a_m + \Delta_{15} - \Delta_{16}),$$

$$c_7 = \frac{\Delta_{19}\Delta_{21} + \Delta_{22}\Delta_{18}}{\Delta_{17}\Delta_{21} + \Delta_{20}\Delta_{18}}, c_8 = \frac{\Delta_{19}\Delta_{20} - \Delta_{22}\Delta_{17}}{-\Delta_{18}\Delta_{20} - \Delta_{21}\Delta_{17}},$$

$$\Delta_{12} = -A_1[\delta_{50} + \delta_{51} + \delta_{52} + \delta_{53}],$$

$$\delta_{50} = \frac{\delta(E_4 + E_3)}{(\delta^2 - a^2)}(a_1 \cosh \delta + \sinh \delta),$$

$$\delta_{51} = [\frac{E_4}{(\delta^2 - a^2)} - \frac{2\delta^2 E_4}{(\delta^2 - a^2)^2}](\cosh \delta + a_1 \sinh \delta),$$

$$\delta_{52} = \frac{\zeta(E_4 + E_3)}{(\zeta^2 - a^2)}(a_3 \cosh \zeta + a_2 \sinh \zeta),$$

$$\delta_{53} = [\frac{E_4}{(\zeta^2 - a^2)} - \frac{2\zeta^2 E_2}{(\zeta^2 - a^2)^2}](a_2 \cosh \zeta + a_3 \sinh \zeta),$$

$$\Delta_{13} = \hat{T}\left[\frac{E_{3m} a_4}{(\eta_m^2 - a_m^2)} - \frac{2E_{4m}\eta_m a_5}{(\eta_m^2 - a_m^2)^2} + \frac{E_{3m} a_6}{(\psi_m^2 - a_m^2)} - \frac{2E_{4m}\psi_m a_7}{(\psi_m^2 - a_m^2)^2}\right],$$

$$\Delta_{14} = \frac{E_3}{(\delta^2 - a^2)} - \frac{2\delta a_1 E_4}{(\delta^2 - a^2)^2} + \frac{a_2 E_3}{(\zeta^2 - a^2)} - \frac{2\zeta a_3 E_4}{(\zeta^2 - a^2)^2},$$

$$\Delta_{15} = [\frac{E_{4m}}{(\eta_m^2 - a_m^2)} - \frac{2\eta_m^2 E_{4m}}{(\eta_m^2 - a_m^2)^2}]a_4 + \frac{\eta_m a_5 E_{3m}}{(\eta_m^2 - a_m^2)} + \Delta_{150}$$

$$\Delta_{150} = [\frac{E_{4m}}{(\psi_m^2 - a_m^2)} - \frac{2\psi_m^2 E_{4m}}{(\psi_m^2 - a_m^2)^2}]a_6 + \frac{\psi_m a_7 E_{3m}}{(\psi_m^2 - a_m^2)}$$

$$\Delta_{16} = \frac{E_3 \delta a_1 + E_4}{(\delta^2 - a^2)} - \frac{2E_4 \delta^2}{(\delta^2 - a^2)^2} + \frac{E_3 \zeta a_3 + E_4 a_2}{(\zeta^2 - a^2)} - \frac{2a_2 E_4 \zeta^2}{(\zeta^2 - a^2)^2},$$

$$\Delta_{17} = \cosh a_m, \Delta_{18} = \sinh a_m, \ \Delta_{19} = -[\delta_{54} - \delta_{55} + \delta_{56} - \delta_{57}]$$

$$\delta_{54} = \frac{(E_{3m} - E_{4m})}{(\eta_m^2 - a_m^2)}(a_4 \cosh \eta_m - a_5 \sinh \eta_m)$$

$$\delta_{55} = \frac{2\eta_m E_{4m}}{(\eta_m^2 - a_m^2)^2}(a_5 \cosh \eta_m - a_4 \sinh \eta_m)$$

$$\delta_{56} = \frac{(E_{3m} - E_{4m})}{(\psi_m^2 - a_m^2)}(a_6 \cosh \psi_m - a_7 \sinh \psi_m)$$

$$\delta_{57} = \frac{2\psi_m E_{4m}}{(\psi_m^2 - a_m^2)^2}(a_7 \cosh \psi_m - a_6 \sinh \psi_m)$$

$$\Delta_{20} = \hat{T}a \sinh a, \Delta_{21} = a_m \cosh a, \ \Delta_{22} = \Delta_{12} - a(\Delta_{13} - \Delta_{14})\sinh a - (\Delta_{15} - \Delta_{16})\cosh a$$

From the boundary condition (27), we have

$$M_t = -\left[\frac{D^2 W(1) + M_s a^2 S(1)}{a^2 \theta(1)}\right]$$

The TMN is as follows

$$M_{t2} = \frac{-(\Lambda_1 + \Lambda_2)}{a^2(c_5 \cosh a + c_6 \sinh a + \Lambda_5 + \Lambda_6)} \tag{41}$$

Where

$$\Lambda_5 = \frac{(E_4 + E_3)}{(\delta^2 - a^2)}(\cosh \delta + a_1 \sinh \delta) - \frac{2\delta E_4}{(\delta^2 - a^2)^2}(a_1 \cosh \delta + \sinh \delta)$$

$$\Lambda_6 = \frac{(E_4 + E_3)}{(\zeta^2 - a^2)}(a_2 \cosh \zeta + a_3 \sinh \zeta) - \frac{2\zeta E_4}{(\zeta^2 - a^2)^2}(a_3 \cosh \zeta + a_2 \sinh \zeta)$$

Results and Discussion

The TMNs of M_{t1} and M_{t2} for types I and II of TBCs are obtained theoretically in terms of $\hat{d}, \beta, M_s, R_I^*, R_{Im}^*, \hat{\mu}, \tau$ and Q, which are respectively, the depth ratio, the porous parameter, the solute Marangoni number, the modified internal Rayleigh numbers in fluid and porous regions, the viscosity ratio, the solute-diffusivity ratio, and Chandrasekhar number. The thermal Marangoni numbers are drawn as a function of thermal ratio for the set of parameters $a = 2.5, \quad \hat{d} = 0.2, \quad \beta = 1.0, \hat{\mu} = 2, \hat{S} = 1, \tau = \tau_{pm} = 0.25, Q = 10, M_s = 10, R_I^* = 1$, and $R_{Im}^* = 1$ etc.
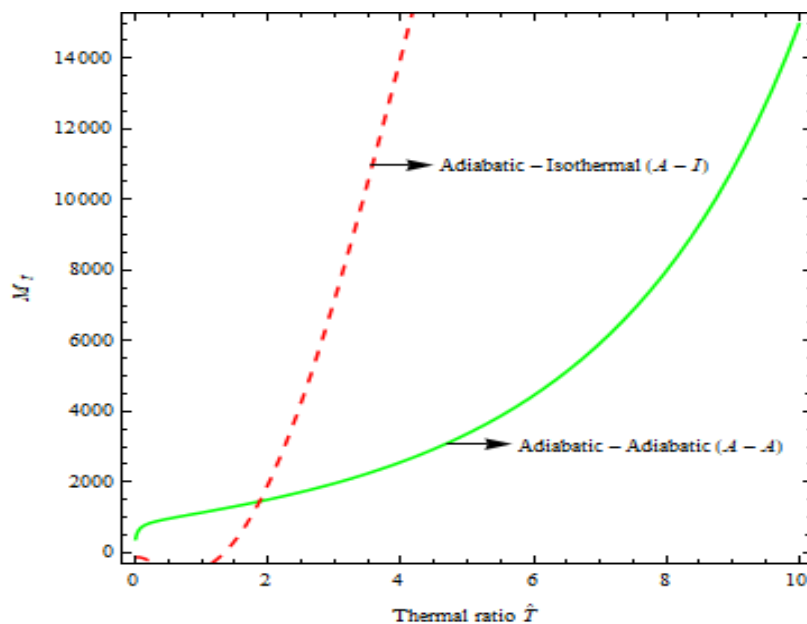
Figure 1-Comparison of thermal Marangoni numbers for type (i) Adiabatic-Adiabatic and type (ii) Adiabatic-Isothermal.

A comparison of the TMNs for types (i) and (ii) TBC is explained by Figure 1, for $a = 2.5, \hat{d} = 0.2, Q = 10, \beta = 1.0, \hat{\mu} = 2, \hat{S} = 1, \tau = \tau_{pm} = 0.25, M_s = 10, R_I^* = 1$ and $R_{Im}^* = 1$ etc., where TMN, M_t is the dependent variable and the thermal ratio $\hat{T}$ is the independent variable. From Figure 1, it is evident that for smaller values of thermal ratio, TMN for Adiabatic-Adiabatic is higher than that for Adiabatic-Isothermal, indicating that, for $\hat{T} < 2$, the TBC type (i) Adiabatic-Adiabatic is suitable for situations where the convection has to be controlled. Whereas for $\hat{T} > 2$, the type (ii) Adiabatic-Isothermal is suitable for the same situations. The other important observation is that in the type (i) Adiabatic-Adiabatic, the TMN increases rapidly as the value of thermal ratio $\hat{T}$ increases, whereas in type (ii) Adiabatic-Isothermal, the TMN slowly increases, reaches a peak value, then decreases with the thermal ratio. The TBCs play an important role in convection, hence choosing containers with appropriate TBC is very important during these processes.

The variation of porous parameter β on TMN is shown in Figures 2a and 2b for two types respectively, for $\beta = 0.1, 1.0, 10.0, 50.0, 100.0$. From Figure 2a, it is observed that the TMN for type (i) Adiabatic-Adiabatic simply increases as the value of thermal ratio is increased. Also, for a fixed value of $\hat{T}$, increasing the value of the porous parameter beta, increases the TMN. Thus, the rise in the porous parameter β is favouring the stability of the system. Hence non-Darcian-Bènard double diffusive magneto-Marangoni convection can be postponed by increasing the porous parameter that is by choosing the size of the pores in the porous layer of the two layer system.
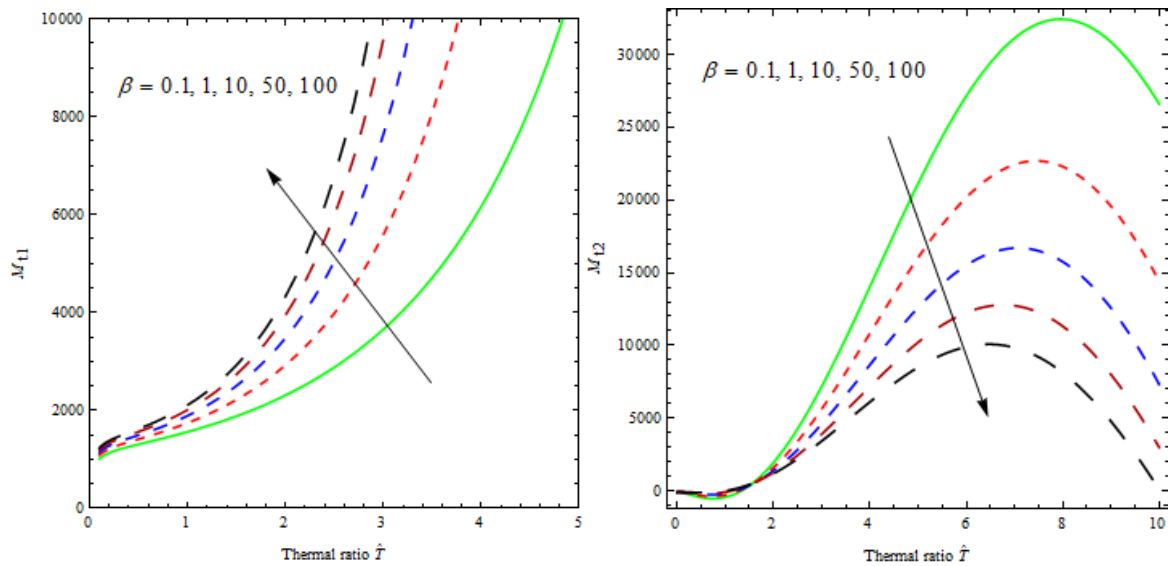
Figure 2- The effects of porous parameter $\beta = 0.1, 1, 10, 50, 100$ on TMN for fixed parameters $a = 2.5, \hat{d} = 0.2, Q = 10, \hat{\mu} = 2, \hat{S} = 1, \tau = \tau_{pm} = 0.25, M_s = 10, R_I^* = 1$ and $R_{Im}^* = 1$
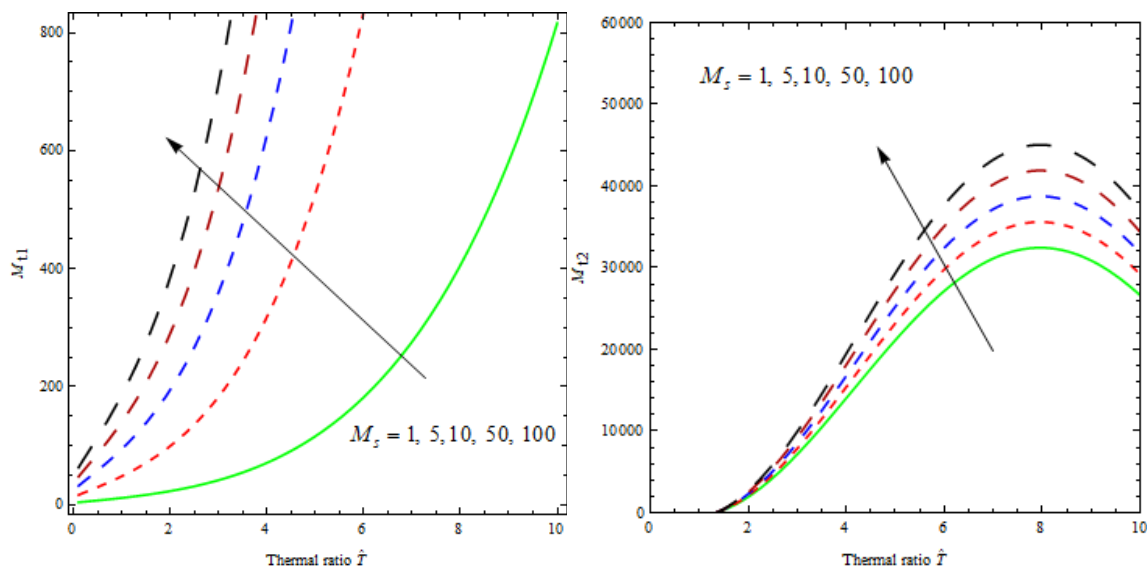

Figure 3- The effects of solute Marangoni number M_s on TMN for fixed parameters $a = 2.5, \hat{d} = 0.2, Q = 10, \beta = 1.0, \hat{\mu} = 2, \hat{S} = 1, \tau = \tau_{pm} = 0.25, R_I^* = 1$ and $R_{Im}^* = 1$

Figure 2b depicts the TMN results for type (ii) Adiabatic-Isothermal TBC. The TMN value increases slowly, reaches its peak, and falls again as the thermal ratio value increases. Also, for a fixed value of thermal ratio $\hat{T}$, as the β value increases from 0.1 to 100, the TMN decreases. The $\hat{T}$ value at which the peak of TMN also shifts towards smaller $\hat{T}$. It is very important to note that increasing permeability means more space for the fluid to move in the porous layer, which is stabilizing for type (i) but destabilizing for the type (ii) TBC. Thus, by merely changing the thermal boundary condition at the upper boundary, one can reverse the effects on the non-Darcian-Bènard double diffusive magneto-Marangoni convection.

Figure 3 demonstrates the effects of solute Marangoni number on the TMN, hence on the non-Darcian-Bènard double diffusive magneto-Marangoni convection. The values of

supplementary parameters are fixed and they are   and , while the values of the solute Marangoni number are . It is quite appealing to note that, for both cases of TBC, the behavior of the eigenvalue is qualitatively similar for all thermal ratios as well as upon increasing the value of solute Marangoni number. The diverging curves reveal that the effect of the solute Marangoni number is drastic for larger values of thermal ratios. For a fixed value of thermal ratio , the increase in the value of solute Marangoni number increases the TMN. Hence, the non-Darcian-Bènard double diffusive magneto-Marangoni convection is postponed and hence stabilize the system.
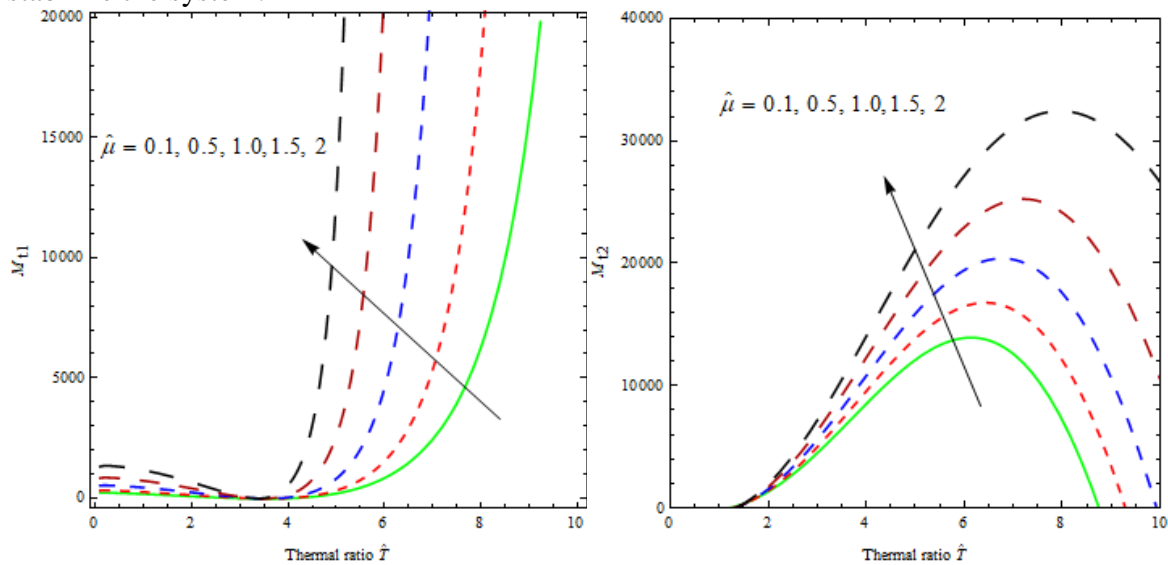

Figure 4- The effects of viscosity ratio $\hat{\mu} = 0.1, 0.5, 1.0, 1.5, 2$ on TMN for fixed parameters $a = 2.5, \hat{d} = 0.2, Q = 10, \beta = 1.0, \hat{S} = 1, \tau = \tau_{pm} = 0.25, M_s = 10, R_I^* = 1$ and $R_{Im}^* = 1$
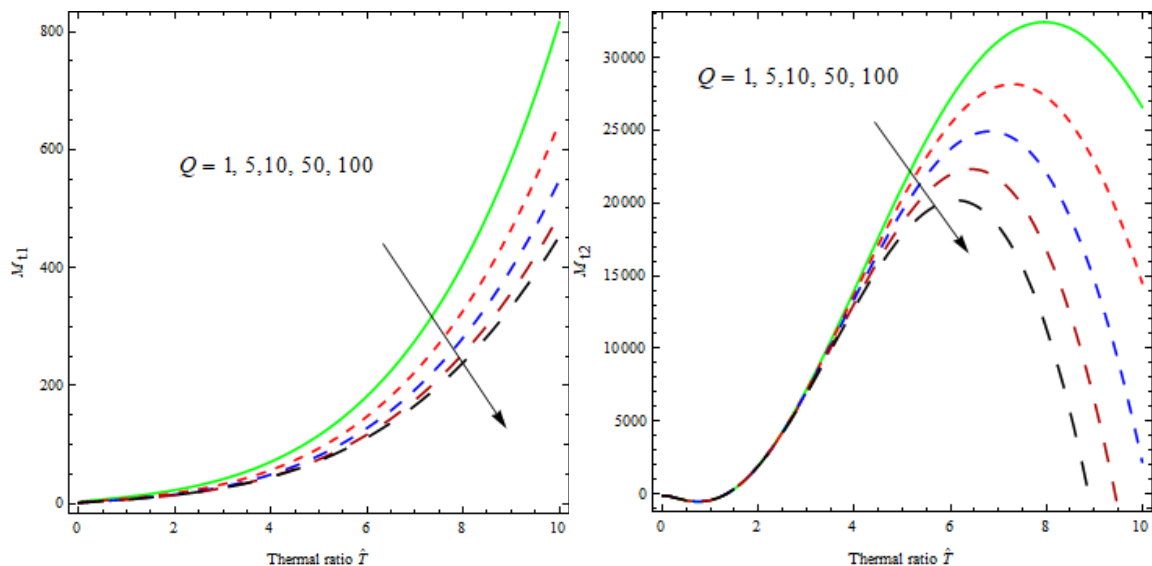

Figure 5- The effects of Chandrasekhar number $Q = 1, 5, 10, 50, 100$ on TMN for fixed parameters $a = 2.5, \hat{d} = 0.2, \beta = 1.0, \hat{\mu} = 2, \hat{S} = 1, \tau = \tau_{pm} = 0.25, M_s = 10, R_I^* = 1$ and $R_{Im}^* = 1$

The effects of viscosity ratio $\hat{\mu}$ on the TMN is shown in Figure 4 for $\hat{\mu} = 0.1, 0.25, 0.50, 0.75, 1.0$. The values of the other parameters are $a = 2.5, \hat{d} = 0.2, \beta = 1.0, Q = 10,$ $\hat{S} = 1, \tau = \tau_{pm} = 0.25, M_s = 10, R_I^* = 1$, and $R_{Im}^* = 1$. For both types of TBCs, the curves are diverging, which indicates that the impact of $\hat{\mu}$ is stronger for higher thermal ratios. For a fixed value of thermal ratio, the increase in the ratio of the effective viscosity of the fluid in the porous region to that in the fluid region leads to an increase in the TMN value. Hence, the non-Darcian-Bènard double diffusive magneto-Marangoni convection is postponed. That is, as the effective viscosity of the fluid in the porous layer is increased, the two layer system is getting stabilized for higher thermal ratio values.

The effects of Chandrasekhar number Q on the TMN is shown in Figure 5 for $Q = 1, 5, 10, 50, 100$. The values of the other parameters are $a = 2.5, \hat{d} = 0.2, \beta = 1.0, \hat{\mu} = 2,$ $\hat{S} = 1, \ \tau = \tau_{pm} = 0.25, \ M_s = 10, R_I^* = 1$, and $R_{Im}^* = 1$. For both types of TBCs, the curves are diverging, which indicates that the impact of magnetic field, i.e. Chandrasekhar number, is stronger for higher thermal ratios. For a fixed value of thermal ratio, the increase in the ratio of Q leads to a decrease in the TMN. Hence, the non-Darcian-Bènard double diffusive magneto-Marangoni convection is preponed. The applied magnetic field, which is usually thought as stabilizing, is destabilizing in this type. This may be due to the presence of a second diffusing component.
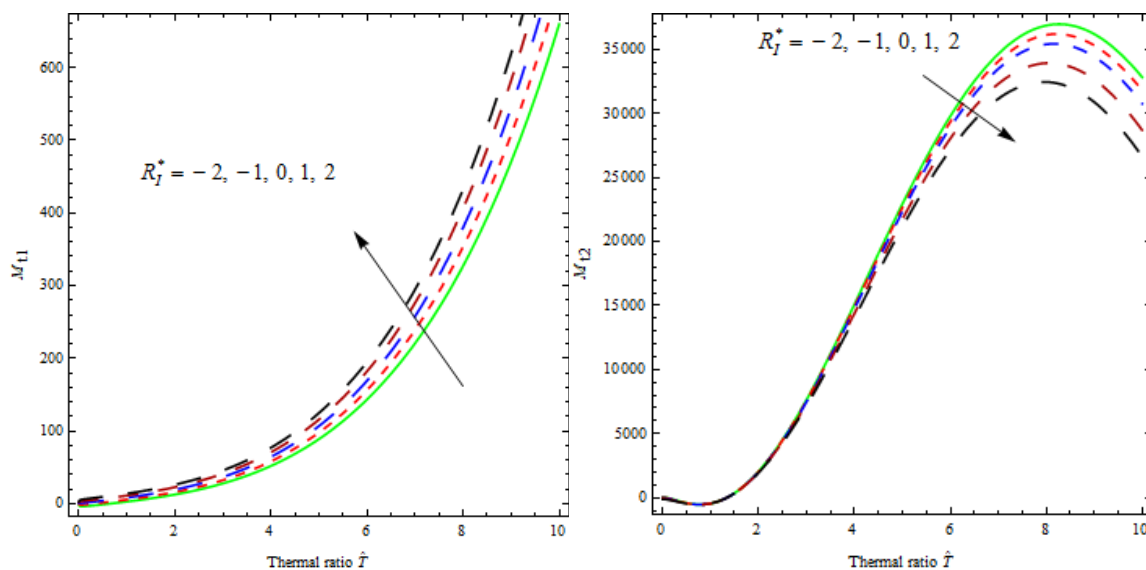

Figure 6- Effects of modified internal Rayleigh number $R_I^* = -2, -1, 0, 1, 2$ for the fluid region on TMN for fixed parameters $a = 2.5, \hat{d} = 0.2, Q = 10, \beta = 1.0, \hat{\mu} = 2, \hat{S} = 1, \tau = \tau_{pm} = 0.25, M_s = 10$ and $R_{Im}^* = 1$

The core of heat source/sink in the fluid region reflects the significance of the modified internal Rayleigh number R_I^* =-2, -1, 0, 1, 2 as shown in Figure 6. The values of the other parameters are $a = 2.5, \hat{d} = 0.2, Q = 10, \beta = 1.0, \hat{\mu} = 2, \hat{S} = 1, \tau = \tau_{pm} = 0.25, M_s = 10$ and $R_{Im}^* = 1$. The negative value of R_I^* denotes the sink and the positive value implies the source. The diverging curves for both types of TBCs reveal that the impact of R_I^* is stronger for higher values of thermal ratio. For a fixed thermal ratio, the increase in the value of internal

Rayleigh number (sink to source) leads to an increase in the TMN value for type (i) TBC, whereas it decreases this value for type (ii). Hence, higher values of R_I^* are suitable for the situations controlling the non-Darcian-Bènard double diffusive magneto-Marangoni convection for type (i) TBC, whereas they augment this convection for type (ii).
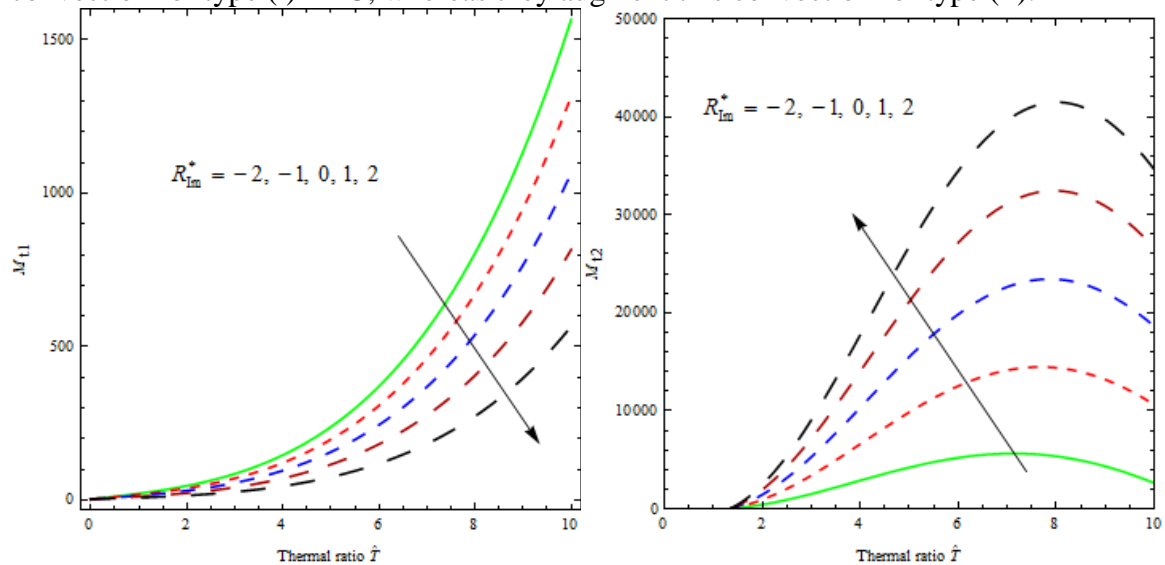

Figure 7- Effects of modified internal Rayleigh number $R_{Im}^* = -2, -1, 0, 1, 2$ for the porous region on TMN for fixed parameters $a = 2.5, \hat{d} = 0.2, Q = 10, \beta = 1.0, \hat{\mu} = 2, \hat{S} = 1, \tau = \tau_{pm} = 0.25, M_s = 10$ and $R_I^* = 1$
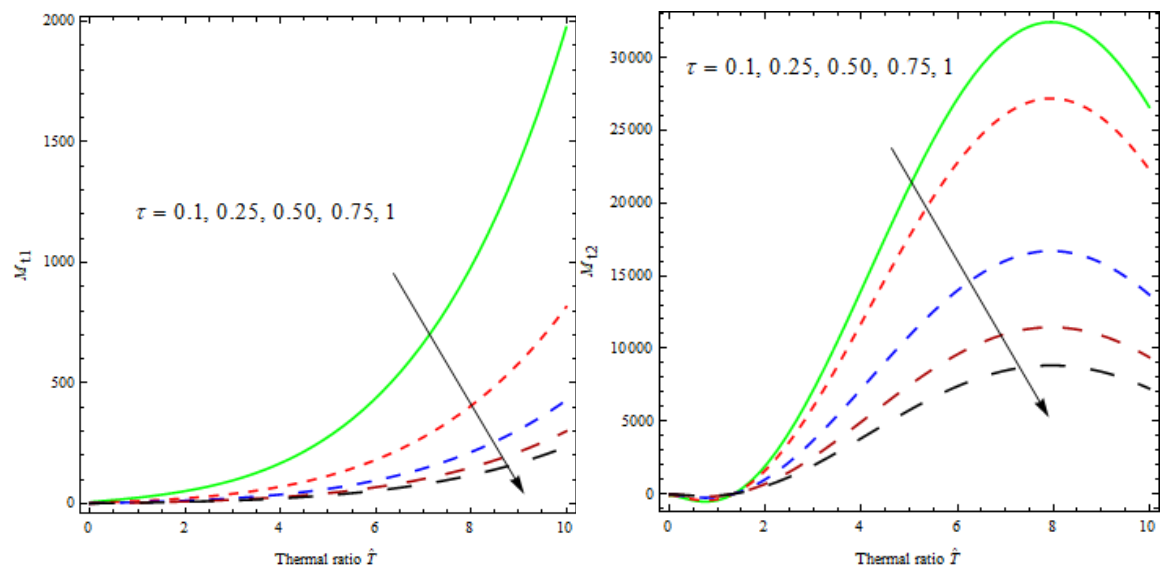

Figure 8- Effects of solute-diffusivity ratio $\tau = 0.1, 0.25, 0.50, 0.75, 1$ on TMN for fixed parameters $a = 2.5, \hat{d} = 0.2, Q = 10, \beta = 1.0, \hat{\mu} = 2, \hat{S} = 1, \tau_{pm} = 0.25, M_s = 10, R_I^* = 1$ and $R_{Im}^* = 1$

Figure 7 demonstrates the effects of modifying the internal Rayleigh number R_{Im}^* on the stability of the two layer system for $R_{Im}^* = -2, -1, 0, 1, 2$. The values of the other parameters are $a = 2.5, \hat{d} = 0.2, Q = 10, \beta = 1.0, \hat{\mu} = 2, \hat{S} = 1, \tau = \tau_{pm} = 0.25, M_s = 10$ and $R_I^* = 1$. The diverging curves for both the cases of TBCs reveal that the impact of R_{Im}^* is stronger for higher values

of thermal ratios. For a fixed thermal ratio, the increase in the value of modified internal Rayleigh number, which occurs from the sink to the source in the porous layer, leads to an increase in the TMN. Hence, larger numbers of R_{Im}^{*} are suitable for the situations controlling the non-Darcian-Bènard double diffusive magneto-Marangoni convection for type (ii) TBC. For a fixed thermal ratio, the increase in the value of modified internal Rayleigh number, which occurs from the sink to the source in the porous layer, leads to a decrease in the TMN. Hence destabilize the system.

The effects of the solute-diffusivity ratio τ on the non-Darcian-Bènard double diffusive Marangoni convection is displayed in Figure 8, for $\tau = 0.10, 0.25, 0.50, 0.75, 1.0$. The fixed parameters are $a = 2.5, \hat{d} = 0.2, Q = 10, \beta = 1.0, \hat{\mu} = 2, \hat{S} = 1, \tau_{pm} = 0.25, M_{s} = 10, R_{I}^{*} = 1$ and $R_{Im}^{*} = 1$. The effect of this parameter is uniform for all thermal ratios for both types of TBCs. For a fixed depth ratio, the increase in the value of diffusivity ratio leads to a decrease in the thermal Marangoni number. Hence, it is an important parameter, the high value of which can accelerate the non-Darcian-Bènard double diffusive magneto Marangoni convection.

Conclusions
The present study has reached several findings. The non-Darcian-Bènard double diffusive magneto-Marangoni convection can be controlled or amplified by choosing the appropriate TBC at the boundaries. For type (i), i.e. Adiabatic-Adiabatic, TBC, the higher values of porous parameter, solute Marangoni number, viscosity ratio, and internal Rayleigh number in the fluid layer, along with the lower values of Chandrasekhar number and the modified internal Rayleigh number in the porous layer, are conducive to the situations that provide more control to the non-Darcian-Bènard double diffusive magneto-Marangoni convection. For type (ii), i.e. Adiabatic-Isothermal, TBC, the lower values of porous parameter, Chandrasekhar number, and modified internal Rayleigh number in the fluid layer, as well as the higher values of solute Marangoni number, viscosity ratio, and modified internal Rayleigh number in the porous layer are conducive to the situations that provide more control to the non-Darcian-Bènard double diffusive magneto-Marangoni convection. Heat source/sink plays an important role in the convection; by choosing an appropriate strength of heat source, the onset of the non-Darcian-Bènard double diffusive magneto-Marangoni convection can be controlled or amplified.

Acknowledgement

Compliance with ethical standards
1) Conflict of interest: Authors declare that they have no conflict of interest.
2) Ethical approval: This article does not contain any studies with human participants or animals performed by any of the authors.

References
[1] Khaled Al-Farhany and A.Turan, "Non-Darcy effects on conjugate double-diffusive natural convection in a variable porous layer sandwiched by finite thickness walls", *International Journal of Heat and Mass Transfer* , vol. 54, no. 13-14, pp. 2868-2879, 2011.
[2] Shivakumara, I.S., Lee, J., Suresh Kumar, S. and Devaraju, N. "Linear and nonlinear stability of double diffusive convection in a couple stress fluid–saturated porous layer", *Arch. Appl. Mech.*, vol. 81, pp. 1697-1715, 2011.
[3] Khaled Al-Farhany and A.Turan., "Numerical study of double diffusive natural convective heat and mass transfer in an inclined rectangular cavity filled with porous medium", *International Communications in Heat and Mass Transfer*, vol. 39, no. 2, pp. 174-181, 2012.

[4]   Mehmood, K., S. Hussain, and M. Sagheer, "Mixed convection flow with non-uniform heat source/sink in a doubly stratified magneto nanofluid", *AIP Advances*, vol. 6, no. 6, pp. 065126, 2016. https://doi.org/10.1063/1.4955157.

[5]   Khaled Al-Farhany and A. Turan., "Double-diffusive of natural convection in an inclined porous square domain generalized model", *Al-Qadisiyah Journal for Engineering Sciences*, vol. 12, no. 3, pp.151-160, 2019.

[6]   Jahirul Haque Munshi, M., Nusrat Jahan, Golam Mostafa., "Mixed convection heat transfer of nanofluid in a Lid-driven porous medium square enclosure with pairs of heat source-sinks", *American Journal of Engineering Research,* vol. 8, no. 6, pp. 59-70, 2019.

[7]   Ali Ahmadpour., Mohammad Reza Daneshvar., M.R. Hajmohammadi and Sepehr Gholamrezaie., "Natural convection of a non-Newtonian ferrofluid in a porous elliptical enclosure in the presence of a non-uniform magnetic field", *Journal of Thermal Analysis and Calorimetry*,2019 https://doi.org/10.1007/s10973-019-0945-3.

[8]   Komala, B and Sumithra, R., "Effects of non-uniform salinity gradients on the onset of double diffusive Magneto-Marangoni convection in a composite layer", *International Journal of Advanced Science and Technology*, vol. 28, no. 15, pp. 874-885, 2019.

[9]   Jha, B.K., Samaila, G. "Effect of heat source/sink on MHD free convection flow in a channel filled with nanofluid in the existence of induced magnetic field: an analytic approach". *SN Appl. Sci.* vol. 2, pp. 1321,2020. https://doi.org/10.1007/s42452-020-3139-8.

[10] Kannan, R. M., and B. Pullepu, "Numerical solutions of double diffusive convective flow past a chemical reactive vertically inclined infinite plate with heat source/sink", *Advances in Mathematics: Scientific Journal,* vol. 9, no. 4, pp. 1623-1636, 2020.

[11] Anurag., A. K. Singh, P. Chandran and N. C. Sacheti, "Effect of Newtonian heating/cooling on free convection in an annular permeable region in the presence of heat source/sink", *Heat Transfer,* 2020. https://doi.org/10.1002/htj.21900.

[12] Sumithra R., R. K. Vanishree and Manjunatha, N., "Effect of constant heat source / sink on single component Marangoni convection in a composite layer bounded by adiabatic boundaries in presence of uniform & non uniform temperature gradients", *Malaya Journal of Matematik*, vol. 8, no. 2, pp. 306-313, 2020.

[13] Sumithra R., Manjunatha N., and Komala B., "Effects of heat source / sink and non-uniform temperature gradients on non-Darcian-Bènard-magneto-Marangoni convection in an infinite horizontal composite layer", *International journal of Applied Engineering Research*, vol. 15, no. 6, pp. 600-608, 2020.

[14] Manjunatha N. and Sumithra R., "Effects of uniform and non-uniform temperature gradients on non-Darcian-Bènard-magneto-Marangoni convection in composite layer in the presence of constant heat source/sink", *Gedrag en Organisatie*, vol. 33, no. 2, pp. 880-896, 2020.

[15] Sumithra, R and Shyamala Venkatraman, "Darcy-Bènard Marangoni convection in a composite layer comprising of couple stress fluid", *International Journal of Applied Engineering Research*, vol. 15, no. 7, pp. 659-671, 2020.